PROCEEDINGS OF SCIENCE

The critical Ising model on an affine plane

Evan K. Owen[a,*] **and Richard C. Brower**[a]

[a] *Boston University, Boston, MA 02215, USA*

E-mail: ekowen@bu.edu, brower@bu.edu

For the 2d Ising model on a triangular lattice, we determine the exact values of the three critical coupling coefficients which restore conformal invariance in the continuum limit as a function of an affine transformation of the triangle geometry. On a torus with a non-trivial modular parameter, we present numerical results showing agreement with the exact CFT solution. Finally, we discuss how this method may be applied to simulate the critical Ising model on curved 2d simplicial manifolds.

The 39th International Symposium on Lattice Field Theory,
8th-13th August, 2022,
Rheinische Friedrich-Wilhelms-Universität Bonn, Bonn, Germany

*Speaker

PoS(LATTICE2022)380

1. Introduction

In a recent paper, Wolff showed that the 2d Ising model can be related to a lattice Wilson-Majorana fermion model via a loop expansion [1]. Using a honeycomb (i.e. regular hexagonal) lattice, it is particularly simple to show that the partition functions of the two models are equivalent. This allows one to identify the exact critical point in both models. More complex generalizations lead to similar results for square and equilateral triangular lattices.

Here, we extend this formalism to include triangular lattices under an arbitrary affine transformation, and their associated dual hexagonal lattices. Special cases of the affine transformation give the familiar result for square and rectangular lattices.

2. Wilson-Majorana Fermion Solution

We begin with general triangular and hexagonal Ising model partition functions,

$$Z^{\triangle} = \sum_{s_n=\pm 1} e^{\,K_1 s_n s_{n+\hat{1}} + K_2 s_n s_{n+\hat{2}} + K_3 s_n s_{n+\hat{3}}}\,, \tag{1}$$

$$Z^{\hexagon} = \sum_{s_n=\pm 1} e^{L_1 s_n s_{n+\hat{1}^*} + L_2 s_n s_{n+\hat{2}^*} + L_3 s_n s_{n+\hat{3}^*}} \tag{2}$$

with 3 independent couplings (K_1, K_2, K_3 for the triangular lattice and L_1, L_2, L_3 for the hexagonal lattice) on the links as illustrated in Fig. 1. In our convention, there is an implied sum over all lattice links. In this section the boundary conditions are arbitrary, but for the numerical simulations in Section 3 we consider a periodic lattice.

Note that at this point, our description contains no information about the geometry of the system. Our goal is to determine the metric of the system (i.e. the lengths of the lattice vectors and the angles between them) at the critical point in the continuum limit. This should be viewed as an emergent property of this strongly-coupled system.

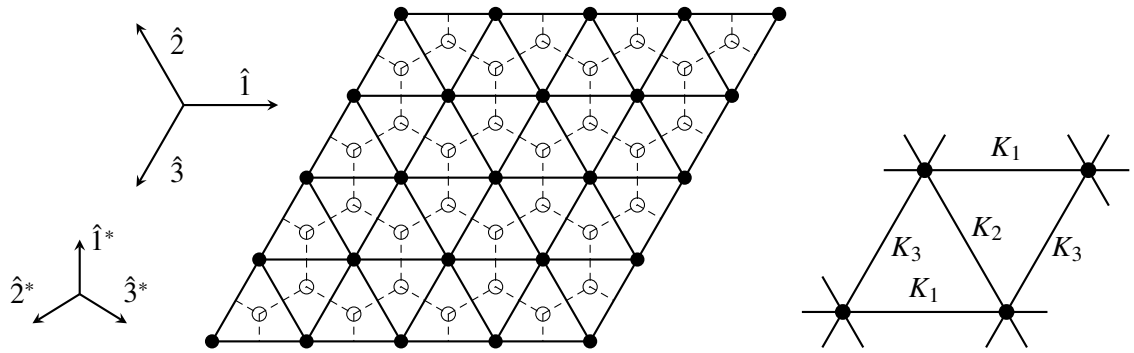

Figure 1: On the left, the triangular graph (black dots) and its hexagonal dual graph (open circles). The triangular lattice has a set of three lattice vectors $\hat{\imath}$ and the hexagonal lattice has a set of corresponding lattice vectors $\hat{\imath}^*$. On the right, the 3 independent couplings assigned to each triangle. Couplings are assigned to the hexagonal lattice similarly.

By using the Star-Triangle relation and Kramers-Wannier duality [2–4], it is known that the critical couplings for these models satisfy the following relations:

$$\sinh 2K_i \sinh 2L_i = 1 \tag{3}$$

$$p_1p_2 + p_2p_3 + p_3p_1 = 1 \quad \text{with} \quad p_i = \exp(-2K_i) \tag{4}$$

$$t_1t_2 + t_2t_3 + t_3t_1 = 1 \quad \text{with} \quad t_i = \tanh(L_i) \tag{5}$$

We would like to determine how these critical couplings are related to the geometric lengths of the triangular and hexagonal links, as required so that the correlation functions of lattice operators have rotational symmetry in the continuum limit. For brevity, we will omit the algebraic and geometric details of the derivation. The interested reader is directed to [5] for more details. A sketch of the proof is given here.

Following Wolff[1], we define a free Wilson-Majorana fermion on the hexagonal lattice with action

$$S[\psi] = \frac{1}{2}\sum_n \bar{\psi}_n\psi_n - \frac{1}{2}\sum_{n,i} \kappa_i\bar{\psi}_n P(\hat{e}_i)\psi_{n\pm\hat{\imath}} \tag{6}$$

where

$$P(\hat{e}_i) = \frac{1}{2}(1 + \hat{e}_i \cdot \vec{\sigma}) \qquad \vec{\sigma} = (\sigma_1, \sigma_2) \tag{7}$$

This differs from the action in [1] in that different hopping parameters κ_i can be chosen for each lattice direction. In the continuum limit, this action can be related to a continuum Majorana fermion action by expanding the field as $\psi_{n\pm\hat{\imath}} = \psi_n \pm a_i\hat{e}_i \cdot \vec{\nabla}\psi_n + O(a_i^2)$.

$$S[\psi] \xrightarrow[a_i\to 0]{} \frac{1}{2}\int d^2x\bar{\psi}_x(\vec{\sigma}\cdot\vec{\nabla} + m)\psi_x \tag{8}$$

The fermion theory has a critical point when $m = 0$ (i.e. the free, massless fermion CFT). In terms of the hopping parameter, this corresponds to $\sum_i \kappa_i = 2$. A solution satisfying this constraint only exists if the hexagonal lattice is the **circumcenter dual** of a triangular lattice. This implies two strong constraints on the subset of hexagonal lattices for which a solution exists:

- Corresponding triangular and hexagonal lattice vectors are orthogonal
- Each hexagon can be circumscribed in a circle (i.e. they are *cyclic hexagons*)

Furthermore, we find that at the critical point the hopping parameters are related to the lattice geometry by

$$\kappa_i = \frac{2\ell_i}{\ell_1 + \ell_2 + \ell_3} \tag{9}$$

where ℓ_i are the lengths of the *triangular* lattice links.

By matching loop expansions of the fermion model and the spin model, it can be shown that the critical couplings K_i and L_i are related to the lattice geometry via

$$\sinh(2K_i) = 1/\sinh(2L_i) = \frac{\ell_i^*}{\ell_i} \tag{10}$$

where ℓ^* are the lengths of the *hexagonal* lattice links.

Eq. (10) is our main result. It is consistent with the special cases of the Ising CFT on a uniform square lattice ($\beta_c = K_1 = K_1, K_3 = 0$) and equilateral triangular lattice ($\beta_3 = K_i$) and the well known critical temperatures: $\beta_3 = \ln(1+2)$ with $\ell_i^*/\ell_i = 1$ and $\beta_3 = \ln(3)/4$ with $\ell_i^*/\ell_i = 1/\sqrt{3}$, respectively. In the next section, we show results of numerical simulations of the critical Ising model on an affine-transformed triangular lattice, which agrees well with continuum results for the 2d Ising CFT.

3. Monte Carlo Simulations

In this section we use our formalism to perform Monte Carlo simulations of two interesting examples of the critical Ising model: the finite modular torus $\mathbb{T}^2$ and the infinite Euclidean plane $\mathbb{R}^2$ (via finite-size scaling). Of course, any simulation must start with a finite lattice, so the traditional test of a CFT on $\mathbb{R}^2$ uses an $L \times L$ periodic lattice (i.e. a torus) in the limit where the longest correlation length ξ satisfies $a \ll a\xi \ll aL$ in units of the lattice spacing a. Technically, this should be a double limit – first the infinite volume limit $L \to \infty$ followed by the approach to the critical surface $\xi \to \infty$ for a CFT or massive theory. However, our affine lattice is also ideal for comparison with the exact finite volume effects of the modular invariance of the torus going to the pseudo-critical surface as we take $L \to \infty$.

For all of our simulations, we perform 2000 thermalization sweeps followed by 50,000 measurement sweeps, with 20 sweeps between measurements. Each sweep consists of 5 Metropolis updates and 3 Wolff cluster updates [6, 7]. With these parameters we find that autocorrelations in our measurements are negligible.

3.1 The Critical Ising Model on the Modular Torus

The first test of our formalism is to embrace the periodic and finite nature of the lattice and compare our data to the Ising model defined on a 2d torus. Traditionally the Ising model is studied only on square and rectangular lattices, but our formalism allows us to simulate the critical Ising model on a torus with arbitrary modular parameter τ.

The modular parameter is a concept familiar to string theorists that is used to parameterize all possible boundary conditions of a torus. Put simply, if the torus is thought of as a tube, the modular parameter is a complex number which parameterizes how the tube is stretched and twisted before its two ends are glued together. The shaded region $\{\tau : |\tau| \geq 1, |\operatorname{Re}\tau| \leq 1/2, \operatorname{Im}\tau > 0\}$ shown in Fig. 2 indicates the fundamental domain of the modular parameter τ. Each value of τ in this region defines a triangle from which we can construct a unique 2d lattice with periodic boundary conditions and the topology of a torus. We have indicated the locations of the equilateral case (τ_{111}), the square case ($\tau_{\square}$), and a representative example of a skew triangle (τ_{456}). The heavy dashed lined is the triangle defined by τ_{456}. The notation τ_{ijk} indicates that the triangle side lengths are proportional to $\{i, j, k\}$.

Without loss of generality, we can sort the triangular lattice lengths so that $\ell_1 \leq \ell_2 \leq \ell_3$. Then the modular parameter in the fundamental domain is

$$|\tau| = \frac{\ell_2}{\ell_1}, \qquad \arg(\tau) = \cos^{-1}(-\hat{e}_1^* \cdot \hat{e}_2^*) \ . \tag{11}$$

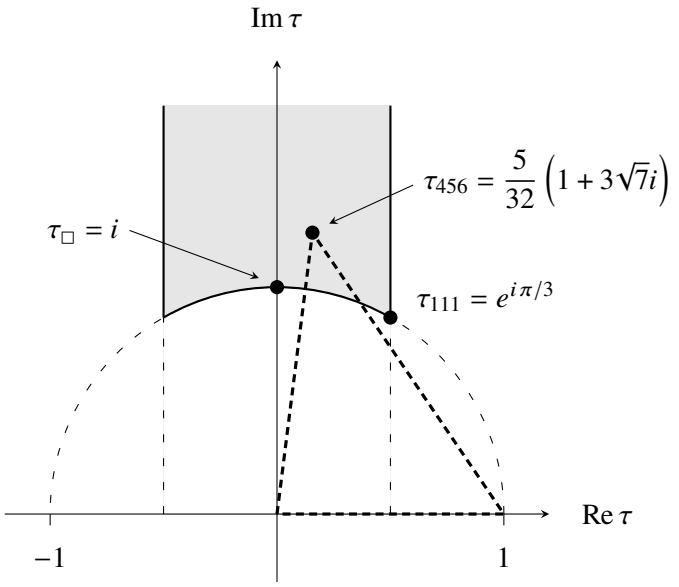

Figure 2: The fundamental domain of the modular parameter τ.

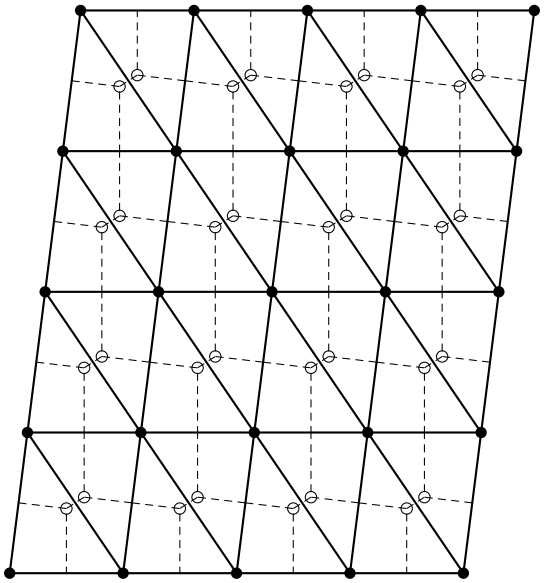

Figure 3: The triangular lattice defined by τ_{456} with $L = 4$. The dashed lines indicate the dual hexagonal lattice with sites at the circumcenter of each triangle.

The lattice is implemented as a refined parallelogram with triangular cells with the appropriate side lengths as shown in Fig. 3.

The continuum two-point function for the critical Ising model on a torus with modular parameter τ is known to be [8]

$$\langle \sigma(0)\sigma(z)\rangle = \left|\frac{\vartheta_1'(0|\tau)}{\vartheta_1(z|\tau)}\right|^{1/4} \frac{\sum_{\nu=1}^{4} |\vartheta_\nu(z/2|\tau)|}{\sum_{\nu=2}^{4} |\vartheta_\nu(0|\tau)|} \tag{12}$$

where $\vartheta_\nu(z|\tau)$ are the Jacobi theta functions and $z = x + iy$ is the separation vector in complex

coordinates. We will use this formula to test our result for the critical Ising couplings on a lattice with an arbitrary modular parameter.

In Fig. 4 we show a contour plot of the continuum 2d Ising spin-spin two-point function on a torus with modular parameter given by Eq. 11 for a triangle with side lengths $\ell_i \propto \{4, 5, 6\}$ and coupling coefficients $\sinh 2K_i = \ell_i^*/\ell_i$, which gives $K_i \simeq \{0.48648, 0.31824, 0.062829\}$. On a triangular lattice, it is convenient to measure the two-point function along the six axes shown. It is sufficient to measure only the bold part of each axis due to the periodicity of the torus.

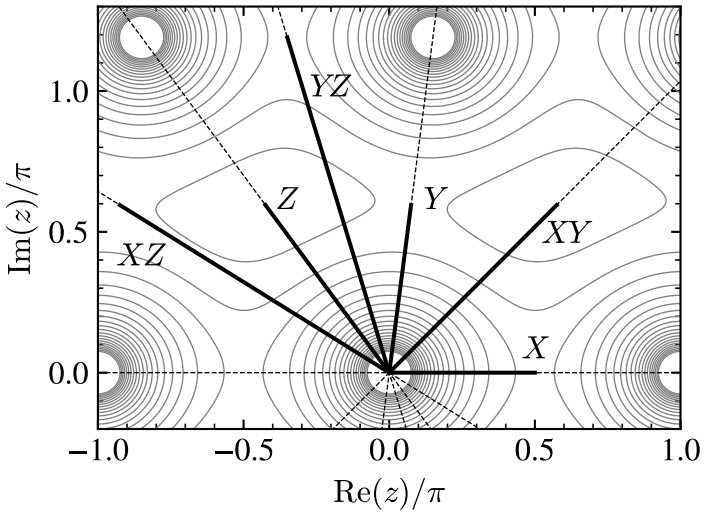

Figure 4: The continuum two-point function in the z-plane with modular parameter τ_{456}, highlighting six axes along which we can easily measure the two-point function on our lattice.

We perform a simultaneous fit to Eq. 12 using lattice data for all six of these axes. The only fit parameter is a single normalization factor. We can see in Fig. 5 that the lattice data is in excellent agreement with the continuum result.

3.2 The Critical Ising Model on the Infinite Plane via Finite-Size Scaling

In this section, we use the same lattice construction as in Sec. 3.1, but now we extract information about the continuum theory on an infinite plane via finite-size scaling. A similar analysis was done for an equilateral triangular lattice in [9]. Our formalism allows us to construct the lattice from triangles with any side lengths. Here, we again use triangles with $\ell_i \propto \{4, 5, 6\}$ because it is sufficiently different from an equilateral, isosceles, or right triangle and will show a clear difference between measurements along different triangle axes.

Again using critical couplings, $\sinh 2K_i = \ell_i^*/\ell_i$, we measure the spin-spin correlation function along the six axes shown in Fig. 4. After scaling the step length for each axis appropriately, the correlation functions collapse onto a single curve at small separation, as shown in Fig. 6. At large separation, wraparound effects cause the correlation function behavior to depend slightly on which axis is being measured.

We perform a finite-size scaling analysis [10–12] to extract the scaling exponent of the first $\mathbb{Z}_2$-odd primary operator, Δ_σ. We measure the magnetic susceptibility $\chi = \langle m^2 \rangle - \langle |m| \rangle^2$ where

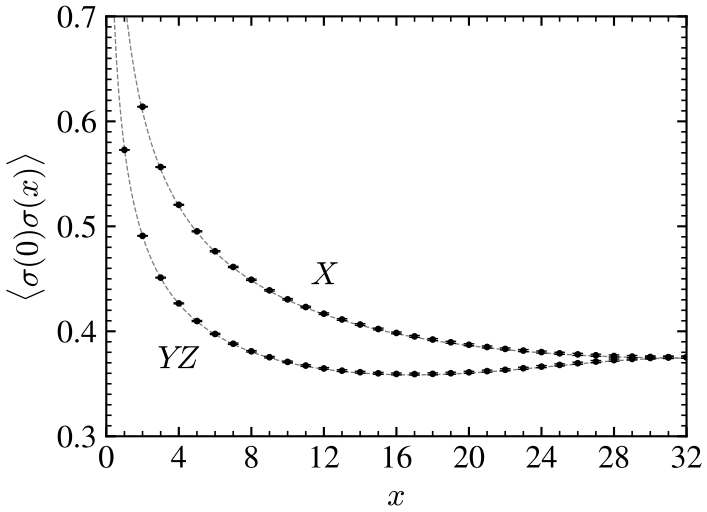

Figure 5: Two-point correlation function measured along the X and YZ axes shown in Fig. 4 for a triangular lattice with $\ell_i \propto \{4, 5, 6\}$ and $L = 64$. The other four axes give similar results. The horizontal axis is the distance measured in lattice steps. The gray lines are the exact correlation function from Eq. 12 and the black points are lattice data.

$m = \sum_i \sigma_i$ is the magnetization. On a finite lattice with characteristic size L, the magnetic susceptibility should scale as $\chi(L) \propto L^{2-2\Delta_\sigma}$. Fitting measurements on $L \times L$ triangular lattices with $L = 8$ up to $L = 256$, we find $\Delta_\sigma = 0.12468(57)$, in excellent agreement with the exact continuum value $\Delta_\sigma = 1/8$. Our fit is shown in Fig. 7.

4. Conclusion

We have shown that the 2d Ising model on a general uniform triangular grid maps to the $c = 1/2$ minimal model on $\mathbb{R}^2$ if the lattice triangulation is given the appropriate affine transformation of the equilateral lattice. This we view as a simple and fortunately analytically soluble example of geometry emerging from a strong coupling quantum field theory at a second order critical point. This affine lattice allowed us to simulate the toroidal geometry and take the continuum limit consistent with exact modular invariance.

We note that the finite element method (FEM) provides a general solution for free conformal theories, defining the map from simplicial complex to continuum CFT on any smooth Riemann manifold in any dimension. While there is much more to consider in this geometric framework, it does suggest possible extensions to other strongly coupled CFTs.

First, in 2d flat space there are many exactly soluble theories which might provide additional examples for this map from lattice action parameters to continuum CFTs. Even beyond soluble models, numerical methods in higher dimensions could be performed to see if similar maps exist in a finite local parameter space, with the hope that the language of projective geometry will suggest an *ansatz* to test.

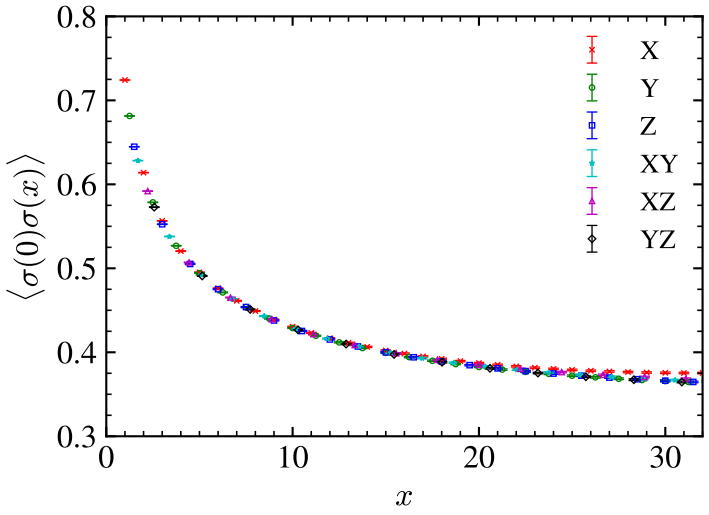

Figure 6: Spin-spin correlation function measured along each of the axes shown in Fig. 4 with distances scaled appropriately based on the lattice lengths ℓ_i. Shown here for $\ell_i \propto \{4,5,6\}$.

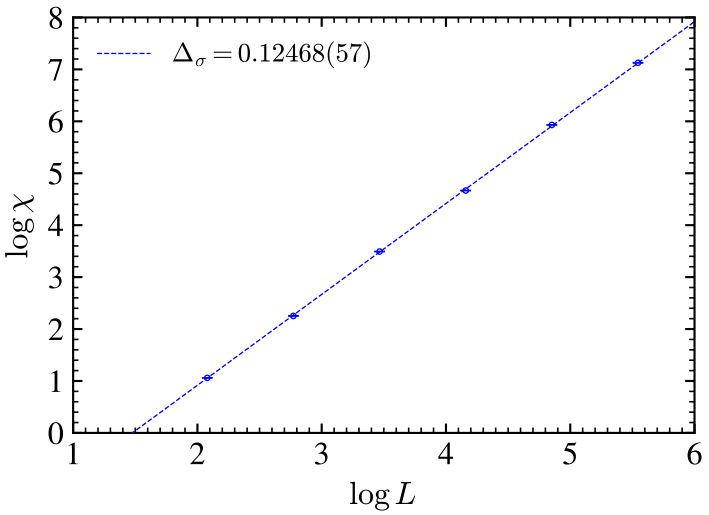

Figure 7: Finite-size dependence of magnetic susceptibility on a lattice with $\ell_i \propto \{4,5,6\}$.

Second, based on our observation that affine transformations provide a general approach to mapping regular lattices in flat space locally to the tangent plane on the curved manifold to $O(a^2)$ in the lattice spacing a, it appears with preliminary numerical investigations that demanding a smooth $O(a^2)$ change in the affine connection between local tangent planes may enable the local determination of a lattice action in a finite parameter space to reach the continuum quantum field theory for the target geometry on the curved manifold. This would be a start at the quantum generalization of the QFE program to strong coupling CFTs. Initial efforts to apply this affine lattice

framework to the tangent plane for radial quantization on $\mathbb{R} \times S^1$ and $\mathbb{R} \times S^2$ appear promising.

We acknowledge the challenges in both of these directions but with deeper insight into the connection between conformal geometry and the simplicial lattice calculus we believe some further progress appears likely.

Acknowledgements

We thank Cameron Cogburn, George Fleming, Ami Katz, Curtis Peterson and Chung-I Tan for helpful discussions. This work was supported by the U.S. Department of Energy (DOE) under Award No. DE-SC0019139 and Award No. DE-SC0015845. The research reported in this work made use of computing and long-term storage facilities of the USQCD Collaboration, which are funded by the Office of Science of the U.S. Department of Energy.

References

[1] U. Wolff, *Ising model as Wilson-Majorana Fermions*, *Nucl. Phys. B* **955** (2020) 115061 [2003.01579].

[2] G. Mussardo, *Statistical field theory: an introduction to exactly solved models in statistical physics*, Oxford Univ. Press, New York, NY (2010).

[3] R. Houtappel, *Order-disorder in hexagonal lattices*, *Physica* **16** (1950) 425.

[4] H.A. Kramers and G.H. Wannier, *Statistics of the two-dimensional ferromagnet. Part I*, *Phys. Rev.* **60** (1941) 252.

[5] R.C. Brower and E.K. Owen, *Ising model on the affine plane*, 2209.15546.

[6] N. Metropolis, A.W. Rosenbluth, M.N. Rosenbluth, A.H. Teller and E. Teller, *Equation of state calculations by fast computing machines*, *Journal of Chemical Physics* **21** (1953) 1087.

[7] U. Wolff, *Collective Monte Carlo updating for spin systems*, *Phys. Rev. Lett.* **62** (1989) 361.

[8] P. Di Francesco, H. Saleur and J. Zuber, *Critical Ising correlation functions in the plane and on the torus*, *Nuclear Physics B* **290** (1987) 527.

[9] L. Zhi-Huan, L. Mushtaq, L. Yan and L. Jian-Rong, *Critical behaviour of the ferromagnetic Ising model on a triangular lattice*, *Chinese physics B* **18** (2009) 2696.

[10] M.E. Fisher and M.N. Barber, *Scaling theory for finite-size effects in the critical region*, *Physical review letters* **28** (1972) 1516.

[11] D.P. Landau, *Finite-size behavior of the simple-cubic Ising lattice*, *Phys. Rev. B* **14** (1976) 255.

[12] K. Binder, *Finite size scaling analysis of Ising model block distribution functions*, *Z. Phys. B* **43** (1981) 119.